Limnol. Oceanogr., 50(3), 2005, 768–778

Pore-water advection and solute fluxes in permeable marine sediments (I): Calibration and performance of the novel benthic chamber system *Sandy*

F. Janssen,[1] *P. Faerber, M. Huettel,*[2] *V. Meyer, and U. Witte*[3]
Max Planck Institute for Marine Microbiology, Celsiusstrasse 1, D-28359 Bremen, Germany

Abstract

This contribution introduces the benthic chamber system *Sandy* that was developed for studying in situ solute fluxes in permeable sandy sediments where advective pore-water transport can dominate solute exchange across the sediment–water interface. The *Sandy* system can be deployed at the seafloor, where it autonomously performs measurements of sediment–water solute fluxes. The innovative features include an insertion mechanism that permits gentle and deep penetration of the chamber into hard consolidated sands with minimum disturbance, and an adjustable stirrer that generates a rotationally symmetric pressure gradient between the center and the circumference of the enclosed sediment surface. In contrast to similar systems, *Sandy* takes advective pore-water exchange into account. Through adjustment of the stirring rate, defined pressure gradients can be established that are similar in shape and magnitude to natural pressure gradients that develop at topographical structures of current-exposed sediment surfaces. Solute fluxes measured in the chamber at a specific ''advective'' stirrer setting can be compared with those obtained at reduced stirring, where pressure gradients are absent and solute exchange therefore is restricted to diffusion and bioirrigation. Rates of pore-water exchange that were determined by means of tracer experiments at different stirrer settings in natural coarse-grained North Sea deposits demonstrate the feasibility of this approach. This permits, for the first time, an evaluation of the contribution of advective exchange to the total interfacial solute flux in situ and makes *Sandy* a valuable tool to study advection-related processes in permeable shelf sediments.

Sandy deposits represent the predominant sediment type in shelf areas worldwide (Emery 1968). The relatively large pore spaces of sands result in high permeabilities that allow for pore-water advection, i.e., mass transport of water across the sediment–water interface and within the sediment itself (Thibodeaux and Boyle 1987). The associated solute exchange between the bottom water and the sediment may exceed molecular diffusion by orders of magnitude and potentially stimulates both chemical reactions and the metabolic activity of biota within the sediment (Huettel and Gust 1992*a*). In laboratory incubations of sandy sediments, this was found to result in enhanced interfacial fluxes of reactive and biologically relevant solutes such as oxygen, nutrients, and heavy metals (Booij et al. 1991; Forster et al. 1996; Huettel et al. 1998). If pore-water advection similarly intensifies metabolic activities and benthic fluxes of sands under natural conditions, it may substantially contribute to organic matter turnover in shelf environments including rates of carbon mineralization, nutrient recycling, and recycled primary production (Boudreau et al. 2001; Huettel et al. 2003). Despite this potential ecological relevance, the significance of advection to solute fluxes in natural permeable sediments is still largely unresolved.

Pore-water advection in the natural environment is typically driven by horizontal pressure gradients at the sediment surface that occur when bottom flow is deflected by topographical structures such as mounds or ripples (Huettel and Gust 1992*a*; Precht and Huettel 2003). Since the pressure gradients scale both with flow velocity and roughness element height (Huettel and Gust 1992*a*; Huettel et al. 1996), rates of advection and their potential significance for biogeochemical processes are closely linked to environmental conditions at the sediment–water interface. Even at a single location, pressure gradients will vary because tidal, wave-, and wind-driven currents as well as sediment topographies constantly change at time scales ranging from seconds to seasons (e.g., Wheatcroft 1994). The tight coupling of pore-water advection rates to the environmental conditions and their spatial and temporal variability makes flux measurements in sands a challenging task.

Measurements of benthic solute fluxes are commonly obtained with benthic chambers by following the evolution of solute concentrations within the water volume that is enclosed together with the underlying sediment. Upon enclosure the ambient currents are replaced by the flow within the chamber water. Depending on chamber design this flow introduces characteristic patterns of shear stress, diffusive

[1] Corresponding author (fjanssen@mpi-bremen.de).
[2] Present address: Florida State University, Department of Oceanography, 0517 OSB, West Call Street, Tallahassee, Florida 32306-4320.
[3] Present address: University of Aberdeen, Oceanlab, Newburgh, Aberdeen AB41 6AA, Scotland, U.K.

Acknowledgments

We thank B. B. Jørgensen for his encouraging support of this work. R. Rimek is thanked for his dedicated work on the design of the *Sandy* system. The construction was very much improved by the technical assistance of A. Cremer, S. Meyer, and T. Kumbier. G. Herz and O. Eckhoff are gratefully acknowledged for manufacturing the system. Thanks are due to R. Reuter, A. Bartholomae, and W. Armonies for sharing their ship time with us. We also thank G. Schüssler, K. Neumann, and C. Wigand for pressure and sulfate measurements and for the fabrication of optodes. F. Aspetsberger helped a lot in the optode measurements. H. Røy and P. Cook are thanked for fruitful discussions on all aspects of this study. Comments by M. Rutgers van der Loeff and an anonymous reviewer strongly improved the manuscript. This study was funded by the Max Planck Society.

boundary layer (DBL) thickness, and differential pressures at the sediment surface (*see* Tengberg et al. 1995 for an overview of chamber designs). Recent intercalibration studies have revealed that chamber-derived diffusive fluxes in muddy sediments of moderate biogeochemical activity are not biased by chamber design and stirring intensity (Tengberg et al. 2004; Tengberg et al. in press). In permeable sediments, on the contrary, fluxes are expected to be strongly dependent on stirrer-induced pressure gradients that develop at the sediment surface also in the absence of sediment topography due to centrifugal forces in chamber water flow cells (Glud et al. 1996). Similar to pressure gradients at current-exposed topographical features, these stirrer-induced gradients result in pore-water advection that circulates the overlying water through the sediment (Huettel and Gust 1992*b*). Patterns and magnitude of the pressure gradients and rates of the ensuing advective exchange in the chambers are hard to predict. They depend on chamber geometry as well as on stirrer design (e.g., rotating stirrer bars, discs, paddle wheels, or circulation pumps), and stirrer orientation (e.g., pressures are higher in horizontally than in vertically stirred chambers) (Tengberg et al. 2004; Tengberg et al. in press). Benthic fluxes that are measured with chambers in the presence of undefined pressure gradients are potentially biased and hence of limited use (Booij et al. 1991; Glud et al. 1996; Jahnke et al. 2000). At a given chamber design, however, the pressure gradient that is generated by the stirring in the chamber is a direct function of stirring rate (Tengberg et al. 2004). Therefore, if firm knowledge exists on the pressure distribution within the chamber and the relationship between pressure gradient magnitude and stirring rate, then chambers may serve as model systems to study solute transport, biogeochemical processes, and benthic fluxes in undisturbed natural sands under defined conditions of advective transport. Such chambers would allow for incubations at documented or even standardized pressure gradients, which would facilitate comparisons of fluxes obtained in different sandy environments. In addition, sediments at a given site could be exposed to changing pressure settings in order to investigate how biogeochemical processes and benthic fluxes depend on the intensity of advective transport. Furthermore, if knowledge of the in situ bottom flow velocities and sediment surface topographies allows an estimation of typical in situ pressure gradients, the stirrer setting can be adjusted so that the pressure gradient inside the chamber and, hence, the exchange rate closely matches environmental conditions. Despite this range of potential applications, we are not aware of any in situ chamber studies of benthic fluxes in permeable sediments that have been performed at defined conditions of advective pore-water exchange. Marinelli et al. (1998) and Jahnke et al. (2000) used chambers with circulation pumps to investigate oxygen and nutrient fluxes and benthic primary production in South Atlantic Bight sediments but gave no details on chamber hydrodynamics and pressure distributions.

In this contribution we introduce the chamber system *Sandy* that performs autonomous chamber incubations in situ with control of advective pore-water transport. It is based on a cylindrical chamber with a centrally mounted, horizontal stirrer disc. Similarly designed laboratory chambers and manually deployed field-going chambers have been used for studies on advective solute transport (Huettel and Gust 1992*b*; Glud et al. 1996), transport and decomposition of particulate organic matter (Huettel and Rusch 2000; Rasheed et al. 2003; Wild et al. 2004), and nutrient recycling (Ehrenhauss et al. 2004). The simple radial symmetry of the chambers has several advantages: the water circulation and the pressure distribution within the chambers as well as the associated pore-water flow field are relatively simple and predictable (Basu and Khalili 1999). The existing pore-water flow trajectories, their depth penetration, and their velocity distribution display strong similarities to those in pore-water flow fields that develop along ripples or mounds that are exposed to bottom flow (Huettel and Rusch 2000). Since the general pressure distribution pattern that is induced by centrally positioned horizontal stirrers is maintained independent of stirrer speed and pressure gradient magnitude (Tengberg et al. in press), the same is true for the pattern of this ''quasi natural'' pore-water circulation.

The novel chamber system *Sandy* is described and characterized with special emphasis on conditions of interfacial solute and pore-water exchange within the chamber. The hydrodynamic properties of the chamber are investigated at different stirrer settings with respect to pressure distribution and DBL thickness. Rates of pore-water exchange that were measured at different stirrer settings in situ are presented to demonstrate the ability of the system to study advection-related processes in the natural environment. Additionally, the performance of the fiberoptic oxygen sensors (''optodes'') employed is assessed, and the novel chamber drive that allows the penetration of consolidated sands is described. Oxygen and nutrient flux data that were obtained with the *Sandy* system in natural sands of different permeabilities are presented in part II of this study (Janssen et al. 2005).

Material and methods

System description—Chamber technique: The *Sandy* system is based on a compact, self-contained chamber module (Fig. 1a). Two of these modules are attached to a stainless steel tripod that is further equipped with four syringe water samplers (Fig. 1b). Details on the tripod and the syringe water samplers can be found in Witte and Pfannkuche (2000). At the moment the frame arrives at the seafloor, the chamber is situated approximately 220 mm above the sediment surface (Fig. 2a). The cylindrical stainless steel chamber (200 mm diameter, 2 mm wall thickness) is closed from below with a piston that later serves as the chamber lid and holds the stirrer disc. An external collar surrounds the chamber at the same vertical level. As the drive motor starts turning the threaded rod, the chamber, the collar, and the lid slowly approach the sediment. Once the lid reaches its ultimate distance to the sediment (typically 120 mm), the chamber and the chamber drive are released (all gray parts in Fig. 1a). Driven by its weight, the chamber slides down (Fig. 2b) and penetrates the upper sediment layer within approximately 1 s. As the lid keeps its distance to the sediment, the enclosure takes place without displacing the overlying

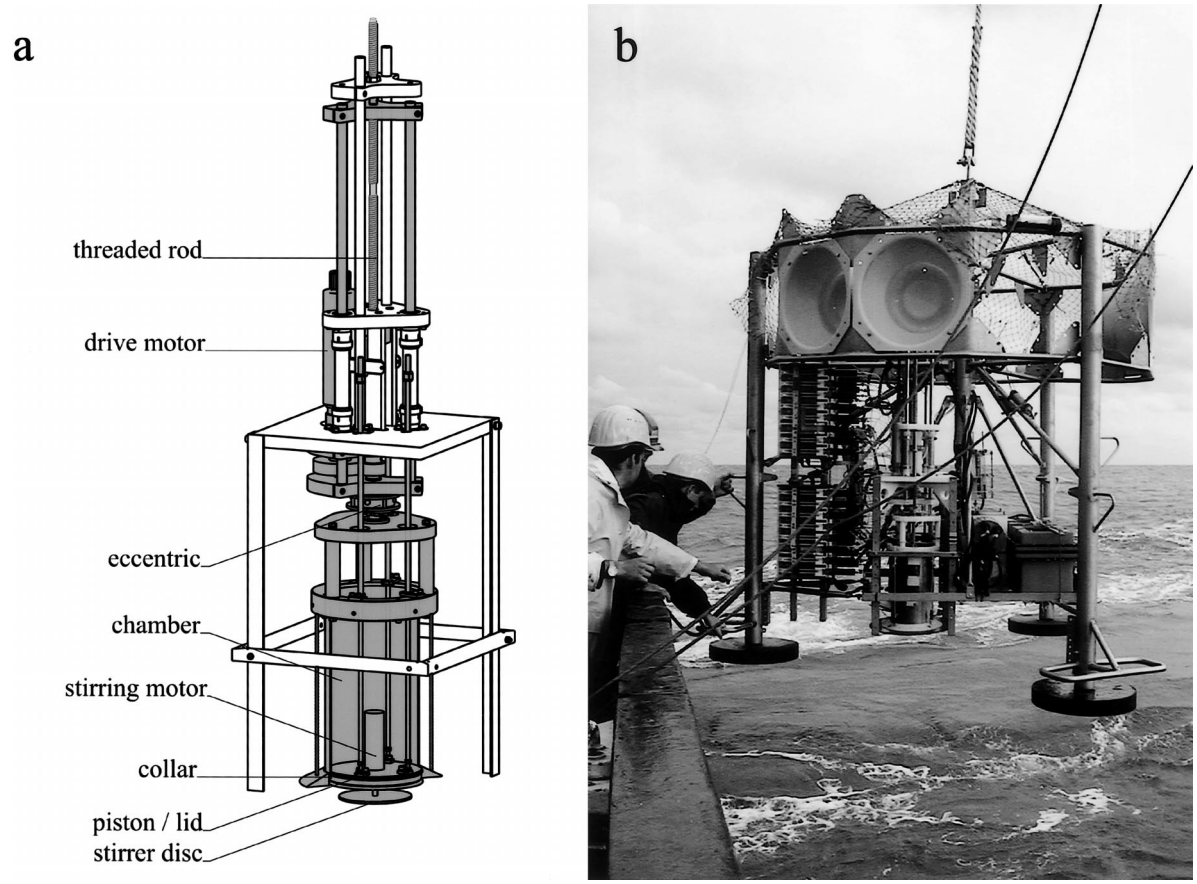

Fig. 1. (a) Details of the *Sandy* chamber module. All gray parts move up and down with the chamber drive. Parts of the chamber wall and the collar are removed to show the piston/lid and the stirrer. The chamber has an inner diameter of 200 mm. The stirrer disc (156 mm diameter × 4 mm) is mounted 20 mm below the lid. The parts consist either of stainless steel (chamber, rods, nuts, pressure housing, frame) or of plastic (mainly Homopolymer Acetal [POM] and Polycarbonate: lid, stirrer disc, guides, mountings). (b) The entire chamber system containing two *Sandy* modules and four syringe water samplers (to the left of the chamber modules).

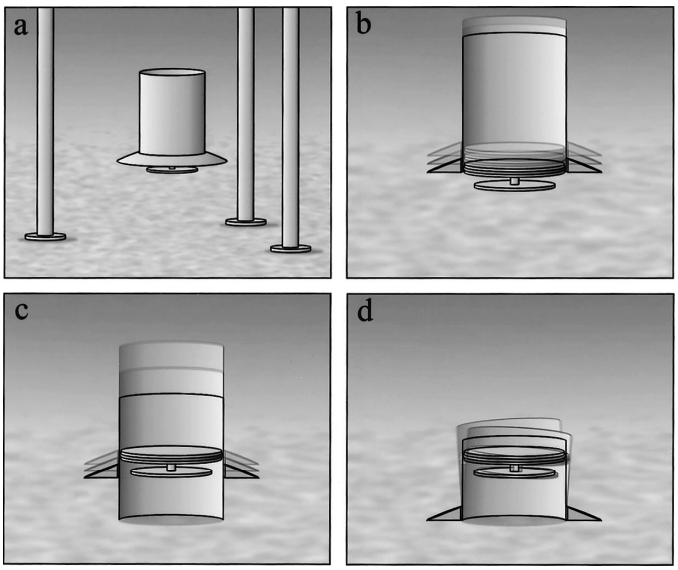

Fig. 2. (a–d) Schematic of a chamber deployment. In panels b–d the front part of the chamber wall is removed to show the position of the lid. Refer to the text for details.

water (Fig. 2c). While the motor continues to turn the threaded rod, the chamber is slowly forced further down until it arrives at its final depth (with the lower rim typically 150 mm below the surface; Fig. 2d). The penetration of the sediment is facilitated by the eccentric that moves the upper part of the chamber along a small circular path resulting in a slight rotating tilting of the chamber of about 1° in all directions. After the incubation, the drive motor turns in the opposite direction pulling the chamber out of the sediment. The initial chamber to sediment distance, the chamber intrusion depth, and the lid to sediment distance can all be adjusted.

The stirrer disc is coupled to the stirrer motor through a magnetic clutch. The speed of the stirrer disc is permanently monitored by means of a photoelectric sensor and adjusted according to the selected stirring rate by a central electronic unit that controls the entire system, performs optode measurements, and logs the data. To minimize flow obstructions within the chamber, sampling ports and sensors are inserted into a water circuit (gastight Viton® tubing, 30 ml total volume) with inflow and outflow located next to the stirrer disc (Fig. 3). The circuit is permanently flushed with chamber water at 20 ml min^{-1} by means of a peristaltic pump (Mas-

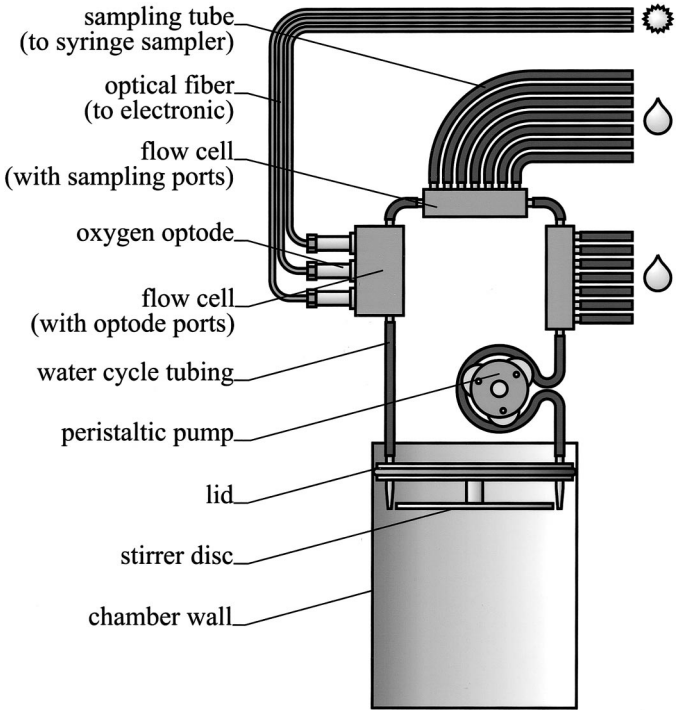

Fig. 3. Schematic of the chamber water circuit (not to scale) including flow cells with ports for the connection of three optodes and two syringe water samplers.

terflex® standard pump head). Since the sampling ports are positioned close to the syringe samplers, sampling tubes of 500 mm length (tube dead volume 2.6 ml or ~5% of syringe volume) are sufficient to connect the syringes to the water circuit.

Optode setup: The fiberoptic optode setup consists of a light-emitting diode (LED) (20 KHz intensity modulated) for excitation of the oxygen sensitive ruthenium fluorophore at the tip of the optode (multimode 100/140 μm), a wavelength division fiber coupler, and a photomultiplier tube (PMT) (Klimant et al. 1995; Glud et al. 1999). The measurements are based on the luminescence lifetime of the fluorophore, which changes as a function of the ambient oxygen concentration. The lifetime is detected as a phase angle shift between the oscillation of the excitation light and the luminescence of the fluorophore as described by Holst et al. (1997). The actual phase angle readings (0 to 2 π) are stored once every second at 14-bit resolution. A custom-built fiberoptic rotary switch switches between six optodes (three replicate optodes per chamber). Fluorescent paint of negligible lifetime at an additional position of the switch serves as an internal reference to correct for phase angle changes due to warm-up of the LED and the PMT.

Hydrodynamic properties of the chamber—In order to characterize radial pressure distributions and hydrodynamics in the *Sandy* chamber, we performed laboratory measurements in acrylic chambers of exactly the same size and geometry. Special emphasis was put on two particular stirrer settings: stirring continuously at 40 rpm (subsequently referred to as ''advective'' stirrer setting) and intermittently at 20 rpm (15 s clockwise, 15 s pause, 15 s counterclockwise, 15 s pause. . .; ''nonadvective'' stirrer setting). The chambers were filled with deionized water of room temperature (18°C), and, unless otherwise stated, measurements were performed at 100 mm distance between the lower surface of the stirrer disc and the bottom (120 mm overlying water height).

Radial pressure gradient: The radial pressure gradient was determined for a range of stirring rates (including the advective and nonadvective stirrer setting) and at different stirrer to bottom distances. The chambers were closed from below by a plastic bottom, covered by a 250-μm nylon mesh to mimic a roughness comparable to that of sandy sediments. A wet/wet differential pressure transducer (Effa GA 63) was used for sequential pressure measurements between a pressure port drilled through the center of the bottom and six ports aligned along the radius of the bottom as described by Huettel and Gust (1992*b*) and Glud et al. (1996).

Chamber water mixing: The dispersal of a cloud of fluorescent dye of virtually neutral buoyancy (50 mg L^{-1} aqueous sodium fluorescein solution; color index 45350) was monitored at the nonadvective stirrer setting, which represented the lowest investigated mixing intensity. Five bare optic fibers (multimode, 140 μm outer diameter) with uncoated tips were introduced from below through three ports in the gauze-covered plastic bottom (*see Fig. 6* for exact tip positions). The fibers were connected to a fluorometer, which is an intensity-based version of the optode device described above. For the range of concentrations used, the fluorescence scaled linearly with dye concentration. After starting the stirrer, 40 ml of the fluorescent dye was added to the chamber water circuit, which was similar to that of the *Sandy* system, and the dye concentration at the fiber tips was monitored for 1 h.

DBL thickness: The average DBL thickness (z) was assessed using the alabaster dissolution method (Santschi et al. 1991). The bottom of six chambers was covered by a uniform layer of alabaster ($CaSO_4 \times 2H_2O$) (three replicate chambers for the ''advective'' and ''nonadvective'' stirrer setting). After filling the chambers with deionized water, the stirrers were run for 1 d at the respective modes. During the time course of the incubation, 13 samples (3 ml) per chamber were taken from the chamber water circuit. An additional sample was taken from one of the chambers after stirring another 30 d at 40 rpm to determine the sulfate concentration at saturation. Sulfate concentrations were measured with an ion chromatograph (Waters IC-Pak™ Anion column and model 430 conductivity detector). The DBL thickness was then determined by fitting the sulfate concentration time series with an exponential equation that describes the $CaSO_4$ accumulation in an enclosed water volume in relation to the boundary layer thickness (Buchholtz-Ten Brink et al. 1989). The effective molecular diffusivity of SO_4^{2-} at 18°C was taken from Li and Gregory (1974) and corrected for cross-coupled diffusion as described in Santschi et al. (1991).

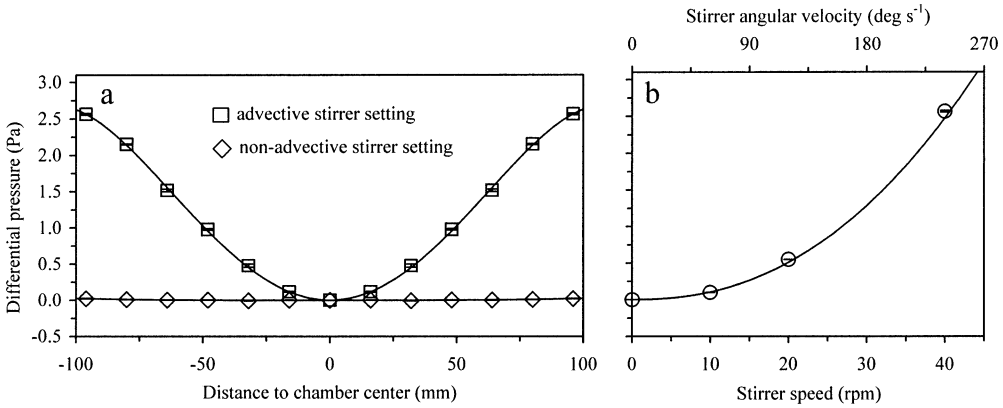

Fig. 4. (a) Radial pressure distribution at the chamber bottom at stirring rates of 40 rpm (continuously; squares), and 20 rpm (intermittent; diamonds). Pressures were measured relative to the center port at six ports along the chamber radius (r = 16 to 96 mm, 16 mm spacing) and mirrored to the opposite side (−16 to −96 mm). The whiskers show standard deviations of three measurements. The line represents a fourth order polynomial fit. (b) The relation between the overall differential pressure (center port to most distant port) and stirrer speed (up to 80 rpm; 80 rpm data point not shown). The curve represents a power function (refer to text for details).

Optode performance—The oxygen concentration within a bottle of freshwater was kept at 100% air saturation by bubbling with air. A peristaltic pump circulated the water between the bottle and two flow cells each containing three of the optodes used for *Sandy* (Fig. 3). The bottle as well as the flow cells were placed in a temperature controlled water bath at 18.2°C. In order to determine the number of consecutive readings that are needed to reach a certain measurement precision, a series of optode readings were conducted with the *Sandy* electronics (4 min for each sensor at 1 Hz). The drift of the optode measurements was inferred from a 24-h measurement series of all six optodes by means of linear regressions. Calibration of the optodes was performed by fitting a modified Stern-Volmer equation (Holst et al. 1997) to luminescence lifetimes measured at eight different oxygen concentrations that were obtained by bubbling the bottle with mixtures of air and nitrogen prepared with a gas mixer.

Results

Hydrodynamic properties of the chamber—Pressure gradient: The rotation of the stirrer disc resulted in a radial pressure gradient with pressures rising from the center to the outer rim of the chamber bottom. The upper curve in the left graph of Fig. 4 shows the pressure gradient at the advective stirrer setting (i.e., at 40 rpm) and 100 mm distance between the lower surface of the stirrer disc and the chamber bottom (d). The overall differential pressure (Δp) between the center and the outer rim of the chamber increased with stirrer speed (right graph). For the stirring rates investigated (10 to 80 rpm), the relationship could be approximated by a power function of the form $\Delta p\ (\omega) = 9.33 \times 10^{-6}\ \omega^{2.28}$ ($r^2 = 0.99$) where ω is the angular velocity in degrees per second.

The pressure gradient was also affected by changes in the disc to bottom distance (Fig. 5). While the general shape was maintained (left graph) the overall differential pressure decreased steadily with increasing distance (right graph). The relation was found to be well represented by the reciprocal power function $\Delta p\ (d) = (8.12 \times 10^{-4}\ d^{1.24} + 0.15)^{-1}$ ($r^2 = 0.99$) where d is the distance in millimeters.

The lower curve in the left graph of Fig. 4 shows the radial pressure distribution at the nonadvective setting (d = 100 mm). The overall differential pressure at this stirrer setting was less than 1% of the differential pressure obtained at 40 rpm. This proportion slightly increased with decreasing disc to bottom distance up to a value of 2.5% at the smallest investigated distance of d = 25 mm.

Mixing: Figure 6 shows the fluorescein concentrations at the respective fiber tips while stirring at the nonadvective stirrer setting. A constant reading at all five tips (i.e., a homogenous dye distribution) was reached within a few minutes after the dye injection was completed.

DBL properties: The fitted exponential equations proved to be good approximations of the measured sulfate concentration time series ($r^2 > 0.97$ in all cases). The corresponding DBL thicknesses (average ± SD) were z = 211 ± 4 and 617 ± 24 μm at the advective and nonadvective stirrer setting, respectively. From these DBL thicknesses the shear velocity u_* (cm s^{-1}) was calculated according to the empirical relationship of Tengberg et al. (2004), which was determined from alabaster dissolution rates and skin friction measurements in stirred chambers:

$$z = 76.18 u_*^{-0.933}$$

This resulted in average shear velocities of 0.34 and 0.11 cm s^{-1}, respectively, at the advective and nonadvective stirrer setting.

Optode performance—Precision: Single oxygen measurements as calculated from individual phase angle readings deviated by up to 3.3% air saturation or 10 μmol L^{-1} from

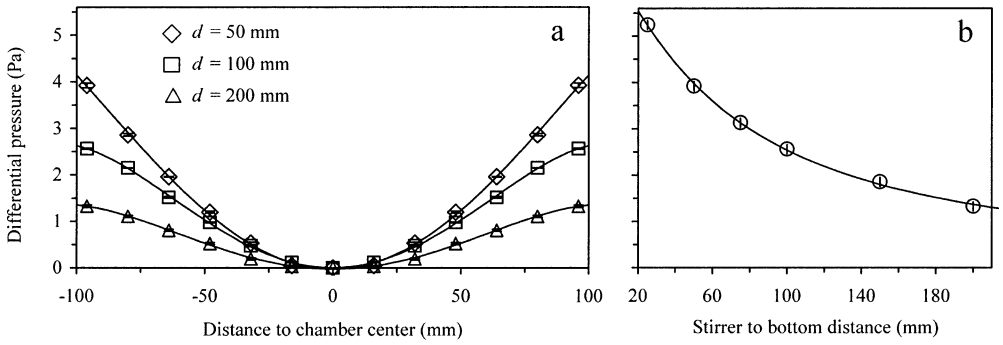

Fig. 5. (a) Radial pressure distribution at the chamber bottom at stirrer to bottom distances of d = 50 mm (diamonds), 100 mm (squares), and 200 mm (triangles) at a stirring rate of 40 rpm (refer to legend of Fig. 4 for details on the arrangement of the pressure ports). The whiskers show standard deviations of three measurements. The line represents a fourth order polynomial fit. (b) The relation between the overall differential pressure (center port to most distant port) and stirrer to bottom distance. The curve represents a reciprocal power function (refer to text for details).

the true oxygen concentration in the aerated bottle (100% or 295.2 μmol L^{-1}). However, calculating averages of 14 successive readings reduced the maximum deviation of all sensors below 1% air saturation.

Drift: During an initial ''warm-up'' period of approx. 6 h, the drift differed considerably between sensors, with a maximum rate of -1.4 μmol L^{-1} h^{-1} for the least stable sensor (determined by linear regression to the first 4 h of measurements). Later on, the rates were both stable and consistent between sensors with an average of 0.21 $\pm$ 0.07 μmol L^{-1} h^{-1} (20–24 h, average of all sensors $\pm$ SD). In a *Sandy* chamber deployment, this drift would result in an underestimate of the actual sediment oxygen uptake of 0.61 mmol m^{-2} d^{-1} (120 mm overlying water height at 100 mm stirrer to bottom distance).

Discussion

In order to obtain realistic flux estimates, it is generally preferable to perform measurements in situ, since physical and biogeochemical sediment properties are altered during sampling and subsequent ageing. This is particularly true with respect to sands because sediment stratification and pore waters are easily lost upon sampling due to the low cohesiveness of the sediment and because sediment biogeochemistry is closely coupled to bottom water hydrodynamics. Current-induced pressure gradients and pore-water advection determine biogeochemical conditions including solute distribution, redox potential, and oxygenation (Ziebis et al. 1996; Huettel et al. 1998; Precht et al. 2004). When sandy sediments are removed from the natural environment, advective solute transport ceases and biogeochemical properties change with time. For example, deep advective oxygenation of freshly retrieved sand cores from the North Sea vanished completely within 1 h (Lohse et al. 1996). In situ incubations avoid sampling artifacts and minimize the delay between enclosure and incubation.

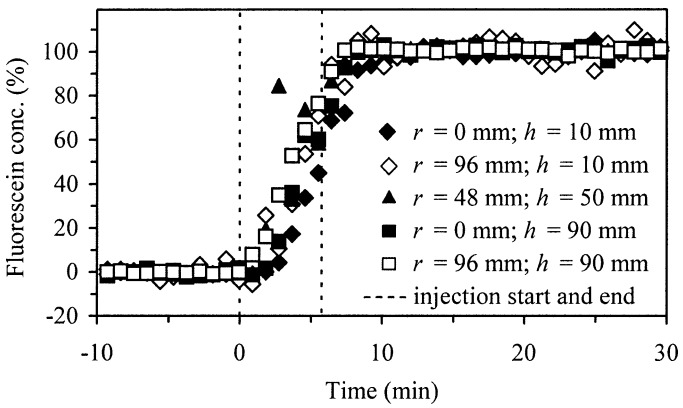

Fig. 6. Fluorescein concentrations (1 min averages) at five different locations within the chamber water relative to the maximum values that were reached after 60 min. The positions of the fiber tips in horizontal (r) and vertical (h) direction are given relative to the center of the bottom (r = 0 mm, h = 0 mm). The vertical lines mark the period of time where the fluorescein injection took place.

Chamber technique—In situ deployments of autonomous benthic chambers today are performed almost routinely down to abyssal depths, and several approaches are available to push the chambers into the sediments (Tengberg et al. 1995). These can be classified as either slowly (damped or motor-driven) or quickly penetrating. In order to develop an approach that suited the specific requirements of deployments on sands in shallow high-energy environments, we carried out extensive test deployments of hand-held chambers in a sandy creek at current velocities of up to 50 cm s^{-1}. Direct and video observations revealed that flow acceleration beneath the chamber led to erosion of the sediment surface if the chamber was placed onto the sediment too slowly and that the sediment surrounding the chamber was washed away within tens of minutes after the chamber penetrated the sediment. A combination of a fast, undamped enclosure of the sediment surface followed by a slow and powerful penetration proved to work best in order to avoid erosion of the sediment surface and to facilitate intrusion to a depth that prevents chamber washout. The tests further showed that flow acceleration beneath the chamber and erosion of the sediment surface prior to enclosure can be reduced if the lower end of the chamber is closed by a bottom

(changing the chamber into a ''solid'' cylinder instead of an open tube) and equipped with an external collar as a flow deflector (Fig. 2a). After the chamber is pushed into the sediment, the same collar, now being flush with the surrounding sediment (Fig. 2d), greatly reduces the washout. These findings were incorporated into the design of the *Sandy* chamber module. A key feature of the construction is the piston-like lid that initially keeps the chamber closed from below to reduce flow acceleration and sediment erosion but maintains its position while the chamber slides down to allow a rapid enclosure of the sediment without displacement of the overlying water. The power needed to accomplish deep penetration of the sediment is greatly reduced by the slightly eccentric movement of the chamber and by the small wall thickness that was possible due to the use of stainless steel as chamber material. A potential overestimate of oxygen fluxes due to an oxygen reduction possibly taking place at the surface of stainless steel chambers (Cramer 1989), was considered to be of minor importance since the main focus of the present version of the instrument was to quantify relative differences in fluxes in response to rates of advection. The effect could be ruled out by coating the inner surface with an insulating compound like polytetrafluorethylen (PTFE). In summary, the chamber system *Sandy* is able to enclose sandy sediments with minimal disturbance of the surface layer and allows flux measurements to be conducted at sandy sites even under harsh conditions that hamper the employment of divers.

Chamber hydrodynamics and conditions of interfacial solute exchange—Once the sediment is enclosed, the hydrodynamic conditions within the chamber water replace the former natural conditions. Knowledge of the stirrer-induced hydrodynamics is important in order to evaluate the potential impact on the measured solute fluxes.

Pressure gradients and advective pore-water exchange: The shape of the pressure gradient corresponds to gradients of similar chambers (Huettel and Gust 1992*b*; Glud et al. 1996). Huettel and Rusch (2000) emphasized the similarity between the pressure distribution that is induced by rotating stirrer discs along the chamber radius of cylindrical chambers and the pressure distribution along topographical features that are exposed to bottom flow. The radial pressure gradient in the cylindrical chamber generates a pore-water flow field that is characterized by velocity gradients, penetration depths, and a central cone-shaped area of funneled pore-water upwelling and release that closely resembles a cross section of the pore-water flow pattern observed under natural current-exposed ripples or mounds (Huettel and Rusch 2000). The shape of the pressure gradient in the *Sandy* chamber was maintained throughout the range of applied stirring rates and hence is independent of the magnitude of the overall differential pressure. The differential pressure was a direct function of the rotational speed of the stirrer disc and of its distance to the sediment. Thus, by selecting the appropriate stirring rate, pressure gradients can be established in the chambers corresponding to natural gradients over a wide range of settings. To our knowledge, the *Sandy* system is the only available instrument to date that permits autonomous incubations under well-defined and adjustable pressure gradients in situ, thus mimicking natural pore-water advection phenomena of various intensities.

The differential pressures that were measured along the impermeable plastic chamber bottom represent maximum values. In the presence of pore-water advection, differential pressures would be relieved to an extent that scales with the sediment permeability. Stirrer-induced pore-water exchange rates at equal stirrer settings, therefore, are not expected to scale linearly with sediment permeability. This agrees with results obtained by Glud et al. (1996), who reported a logarithmic relationship between pore-water exchange and permeabilities in stirred chambers. Natural pressure gradients, developing at given conditions of flow and topography, would be likewise affected by the actual permeability. Incubations at identical stirrer settings on sediments of different permeabilities thus mimic the effect of specific pressure-generating flow and topography conditions rather than that of a specific pressure gradient. If flux measurements at exactly the same pressure gradients are required in different sediments, the stirrer setting can be adjusted for the respective permeabilities.

Solute exchange in the presence and absence of advection: The advective and nonadvective stirrer settings were investigated in more detail. A comparison of fluxes obtained at both settings at the same site in replicate chambers or sequentially within the same chamber allows an investigation of the significance of advective transport as compared with diffusion and bioirrigation. The pressure gradient at the advective setting represents moderate conditions of advective pore-water exchange. The overall differential pressure at that setting (2.9 Pa between the center and the outer rim of the chamber bottom at $d = 100$ mm) equals what has been measured at 10 mm high mounds that were exposed to unidirectional bottom flow at velocities of approximately 20 cm s^{-1} at 10 cm above the bed (Huettel et al. 1996). At the nonadvective setting with an insignificant radial pressure gradient, by contrast, exchange is restricted to diffusion and bioirrigation.

Changing the stirrer setting affects not only the pressure gradient and rates of advective pore-water exchange but also the flow and turbulence properties above the sediment surface. To ensure that differences in benthic fluxes, which are observed between the nonadvective and the advective stirrer setting, are solely attributable to advection, it is necessary to exclude the possibility that the respective solute fluxes or their determination are altered by other processes. The fast dye cloud dispersal confirmed that the nonadvective stirrer setting was efficient in preventing stagnation of the chamber water. This means that even at this gentle stirring mode, changes in solute concentration due to interfacial solute exchange extend to the sampling ports and sensors.

A potential artifact that could bias fluxes at the advective stirrer setting, and that has to be ruled out, is sediment resuspension. Resuspension results in pore-water release from the eroded sediment layer and exposure of formerly covered sediment layers to the overlying water. Oxygen uptake rates in laboratory chambers were found to increase severalfold once the upper sediment layer became resuspended (Glud et

al. 1995). A significant resuspension effect was also described with respect to fluxes of dissolved inorganic carbon, nutrients, dissolved organic carbon, and heavy metals on account of pore-water release and of adsorption/desorption processes (*see* Tengberg et al. (2003*a*), and references therein). In test runs of the acrylic chambers at 40 rpm, we observed no indication of sediment movement (i.e., saltation of sediment grains or sediment accumulation in the chamber center where resuspended particles tend to accumulate), which confirmed that the shear velocity was subcritical for the sediment used (washed and sieved well-sorted fine silicate sand, 220 μm median grain size). Because sands of this grain size are particularly sensitive to erosion (e.g., Hjulström's curve in Sundborg 1956), resuspension is not expected to occur at the advective stirrer setting in sands of any grain size. This is in agreement with the average shear velocity as calculated from the alabaster dissolution experiments at the same setting (0.34 cm s^{-1}). According to the ''threshold conditions for granular material'' (Julien 1995), 2–3 times higher shear velocities are needed to erode fine sand particles.

Diffusive fluxes across the DBL: DBL thicknesses as determined at the advective and nonadvective stirrer setting are both within the range of values that have been reported from shallow-water environments (Glud et al. 1996; Jørgensen 2001) but differed by almost a factor of three. Several authors stressed that chamber-derived diffusive fluxes may be affected by the thickness of the DBL at the surface of the enclosed sediment (e.g., Hall et al. 1989). However, if the chambers, instead of being closed by an impermeable alabaster layer, were deployed on permeable sands (i.e., the sediments the system is intended for) at a stirrer speed of 40 rpm, a DBL would most likely be absent. Oxygen profiling in permeable sands that were exposed to bottom flow indicated the absence of a DBL at the sediment surface even in the absence of surface topography (Forster et al. 1996; Ziebis et al. 1996; Guess 1998). This was attributed to flow across the interface due to advection along minute roughness elements and bottom shear-induced dispersion within the uppermost sediment layer. Diffusive exchange across the sediment surface of sands at the advective stirrer setting is thus most likely not limited by a DBL. This is not an artifact but a natural characteristic of sandy environments that are affected by advection. At the nonadvective setting, on the other hand, a DBL will develop since advection will be absent and dispersion is limited at reduced flow and turbulence conditions. Since the DBL at this setting had a realistic thickness (i.e., 617 μm), an influence on interfacial solute fluxes does not represent an artificial constraint but corresponds to conditions in diffusion-dominated environments. Biogenic solute transport by irrigating activity of the enclosed fauna would add to the respective exchange rates at both stirrer settings.

A DBL effect on the fluxes that would be erroneously attributed to advection might be expected if investigations take place in fine sands of low permeability. In the following the potential effect of the DBL will be discussed with respect to oxygen fluxes as a key parameter of benthic activity. An increase in DBL thickness (z) results in a reduction in the oxygen concentration at the sediment–water interface (C_w), in oxygen penetration depth, and, hence, in diffusive oxygen flux (J). Assuming that steady state conditions are valid and that sediment diffusivity (Ds) as well as rates of oxygen removal from the pore water (R) are constant throughout the sediment depth, the expected difference in oxygen flux at both stirrer settings may be quantified according to Rasmussen and Jørgensen (1992). Rearranging their eqs. (2) and (5) allows the flux to be related to the DBL thickness:

$$J = -zRD_S/D + (z^2R^2D_S^2/D^2 + 2C_wRD_S)^{1/2}$$

with D being the diffusion coefficient in seawater. If diffusive oxygen fluxes of 10, 20, and 30 mmol m^{-2} d^{-1} took place at 40 rpm (average DBL 211 μm), changing to the nonadvective stirrer setting (average DBL 617 μm) is expected to reduce fluxes by 0.54, 2.1, and 4.8 mmol m^{-2} d^{-1} or 5.4%, 10.7%, and 15.9% (T = 15°C, S = 35, C_w = 100% air saturation). The DBL effect, thus, is expected to be highest in sediments of high metabolic activity, which is in agreement to reported experimental results (e.g., Jørgensen and Des Marais 1990). The typical oxygen demand of shelf sediments is generally in the lower portion of this range. Based on a compilation of carbon oxidation rates in shelf sediments, Canfield and Teske (1996) give a median oxygen flux of 13.7 mmol m^{-2} d^{-1}. The diffusive oxygen flux is expected to represent only a fraction of this oxygen demand, since solute exchange by the activity of benthic organisms is considered to significantly contribute to oxygen uptake in shelf sediments (Jahnke 2001). Hence, even in incubations on sediments of low permeability it is unlikely that a DBL effect introduces a significant artifact to the oxygen fluxes. This is in agreement with the results of Tengberg et al. (2004) and Tengberg et al. (in press), who incubated cohesive sediments in different chambers with average DBL thicknesses between 120 and 711 μm and found that differences in fluxes of oxygen and nutrients were small and not attributable to the respective thicknesses of the DBL.

Enclosed sediment topography: Another aspect to consider is the effect that natural topographical features at the enclosed sediment surface (e.g., ripples or mounds) will have on the exchange rates. The rotational flow could induce localized pressure fields and advection around the roughness elements that could possibly add to the pore-water exchange that is induced by the radial pressure gradient. However, an investigation of exchange across sculptured sand surfaces (a sloping surface and a crest and trough with a triangular cross section; all surfaces inclined by 17°) indicated the opposite effect. The concentration decrease of sodium fluorescein tracer dye that was added to the chamber water revealed that the sculptured surfaces generally reduced the interfacial fluxes. Reduction as compared with a smooth and horizontal surface (average of two replicate runs for each surface) was 31.2% (inclined surface), 27.6% (crest), and 10.0% (trough). While investigations of further topographies are certainly advisable, these results indicate that the enclosure of existing topographies reduces the pore-water exchange that makes chamber-derived estimates of the effect of advection on benthic fluxes conservative. A likely explanation for the observed effect is that the roughness elements disturb the reg-

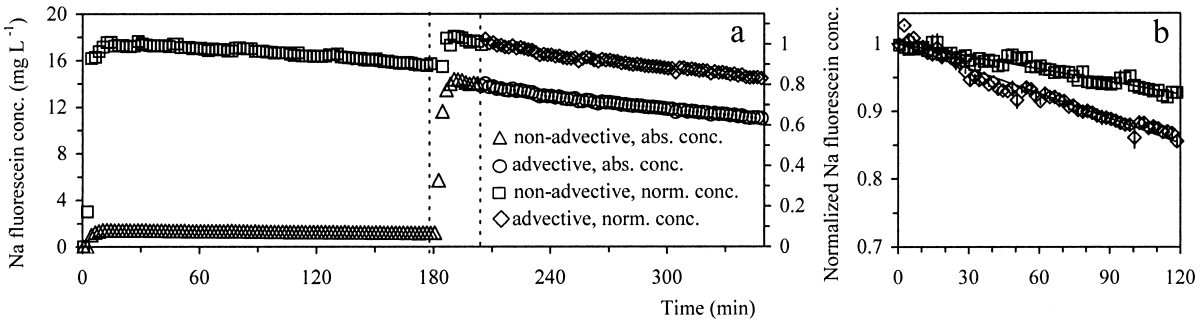

Fig. 7. (a) In situ time series of fluorescein concentrations in the chamber water. 42 ml of a sodium fluorescein solution (100 and 1,000 mg L^{-1}, respectively, adjusted to bottom water density with sodium chloride) were injected into the chamber water at $t = 0$ and $t = 178$ min (first dotted line). The second dotted line marks the time of the change in stirrer setting ($t = 204$ min). Concentrations are expressed as absolute values (triangles and circles) and normalized to the maximum concentration at the beginning of the respective parts (squares and diamonds). The data represent averages of two fluorometer channels. (b) Direct comparison of the normalized fluorescein concentrations of the same incubation during the first 120 min at the advective (diamonds) and the nonadvective stirrer setting (squares). The error bars represent the range of the concentrations as measured by the two channels.

ular flow pattern, which, in turn, reduces the centrifugal forces in the rotating water column and, hence, the differential pressures and exchange rates.

In situ validation: The potential of the *Sandy* system to study the impact of advection on solute fluxes of natural sandy sediments was confirmed by rates of pore-water exchange that were measured at the nonadvective and advective stirrer setting in situ (Fig. 7). Deployments took place on a 16 m deep coarse sand station with a permeability of 7.46×10^{-11} m^2 off the Island of Spiekeroog (German Bight, North Sea; for details on the station *see* Janssen et al. 2005). As described above, a neutrally buoyant sodium fluorescein tracer solution was added to the chamber water to quantify interfacial solute exchange. The same fiber optic fluorometer as in the dye cloud dispersion experiment monitored the decrease in sodium fluorescein concentration in the overlying water over time. The respective slopes show that dye flux to the sediment was smaller at the nonadvective compared with the advective stirrer setting, where pore-water advection resulted in an additional transport of dye across the sediment–water interface. In the advective as well as in the nonadvective phase of the incubation, the tracer decreased fairly linearly with time. This indicates that (1) tracer diffusion at the nonadvective stirrer setting was not substantially hampered by tracer accumulation in the upper sediment layer and that (2) no substantial tracer recirculation took place while stirring at the advective setting. Any strong bias introduced to the rates of tracer decrease in the advective (i.e., the second) phase of the incubation by an outflow of previously stained pore water was ruled out by the application of a tenfold higher tracer concentration before switching the stirring mode. The rates of decrease in tracer concentration at the respective settings can thus be used to calculate the rates of interfacial solute exchange in the presence and absence of advection. The net rate of advective transport (i.e., the difference in rates between both settings) was 91.4 ± 11.5 L m^{-2} d^{-1} (average of the three incubations $\pm$ SD). This agrees with pore-water exchange rates measured with similar chambers in laboratory incubations (Glud et al. 1996). Exposing macrofauna-free sand of a similar permeability (5.69×10^{-11} m^2) to a fivefold lower overall differential pressure (0.52 Pa) than that of our advective stirrer setting resulted in a 5.4 times lower advective pore-water exchange (approximately 17 L m^{-2} d^{-1}; Glud pers. comm.).

Optode performance—The oxygen uptake by marine sediments has been extensively studied and is a commonly used measure of the benthic activity and the total organic matter mineralization in sediments because it represents both aerobic organic matter degradation and anaerobic decay through the oxygen demand for the reoxidation of reduced electron acceptors (Thamdrup and Canfield 2000). Since their introduction to aquatic sciences (Klimant et al. 1995), intensity-based optodes have been used to record oxygen concentrations in benthic chambers (e.g., Glud et al. 1999). A major step forward was the introduction of lifetime-based systems that are less sensitive to fluctuations in light source and in signal intensity (e.g., due to unstable excitation light sources, fiber bending, or changes of the optic properties of the sample) (Holst et al. 1997). Recent deep-sea deployments of a self-contained, lifetime-based optode device similar to the one that is part of the *Sandy* system (Witte et al. 2003) confirmed the general suitability for autonomous chamber deployments. Since the main motivation for the *Sandy* development was an investigation of the oxygen demand of sandy sediments and its response to changing rates of advective pore-water exchange, we tested the system under controlled laboratory conditions to confirm that measurements are sufficiently precise and temporally stable. Averaging 14 replicate phase angle readings proved to reduce the maximum variation between oxygen measurements below 1% air saturation. This precision is within the same range obtained by Winkler titration (i.e., the usual method applied to chamber water samples). Moreover, the three replicate sensor measurements per chamber add further reliability. The main advantage of the sensors in comparison with discrete water samples, however, is the opportunity to monitor the oxygen decrease almost continuously to detect differences in uptake rates in response to rates of advection. A complete cycle of 14 readings of all six optodes including the time needed for switching between optodes takes about 2.5 min, which pro-

vides adequate temporal resolution for chamber deployments that usually last for several hours. The phase angle drift was relatively small and, after the initial warm-up period, linear and similar for all sensors. The bias that would be introduced to absolute fluxes by the long-term drift of the optodes (i.e., an underestimate of the oxygen uptake by 0.61 mmol m^{-2} d^{-1}) is below 5% of the above mentioned typical oxygen demand of 13.7 mmol m^{-2} d^{-1} for shelf sediments (Canfield and Teske 1996). Owing to the fact that the drift was linear, it does not affect relative changes in rates since they might be induced when changing advective settings (e.g., switching between advective and nonadvective stirrer settings). Since the detection of such advection-induced changes in uptake rates is the main purpose of the optodes, the drift problem can be solved by switching on the electronics some hours prior to the deployment, so that drift is stable and linear during the incubation. A promising perspective for future work is the introduction of recently developed macrosize optodes that are reported to display excellent long-term stability (Tengberg et al. 2003*b*).

With the novel *Sandy* system, an instrument is now available that permits in situ studies on the effects of pore-water advection on interfacial fluxes in permeable sediments. The chamber drive minimizes sediment disturbance and chamber washout by combining an undamped enclosure with a deep penetration, thereby facilitating the incubation of sediments in their natural state. Because pressure gradients can be adjusted, it is possible to determine solute fluxes of natural sediments under well-defined conditions of pore-water advection or to quantify changes in these fluxes in response to changes in advective exchange rates. This was demonstrated in situ by a comparison of pore-water exchange rates under an ''advective'' and ''nonadvective'' stirrer setting. Detailed studies of the effect of advection on oxygen uptake as a measure of benthic activity and organic matter mineralization are facilitated by recordings of the oxygen concentration in the overlying water at high temporal resolution via lifetime-based fiberoptic optodes. Scientific questions related to transport and reactions in permeable sediments now can be addressed with the *Sandy* system. An example is the application of a sequence of different stirrer settings in order to investigate the effect of permanently changing pressure gradients encountered when tidal currents interact with a given sediment topography. The addition of dissolved or of particulate organic substrates to the chamber water permits the investigation of the reaction of sands to organic matter pulses. Adding contaminants would help to assess the importance of sands as biofilters and their sensitivity to anthropogenic impacts. Part II of this study focuses on the potential of advection to promote oxygen uptake rates in natural sandy sediments. Results from a fine-, medium-, and coarse-grained sandy site are compared in order to assess the role of advection in sediments of different permeability (Janssen et al. 2005).

References

BASU, A. J., AND A. KHALILI. 1999. Computation of flow through a fluid-sediment interface in a benthic chamber. Phys. Fluids **11:** 1395–1405.

BOOIJ, K., W. HELDER, AND B. SUNDBY. 1991. Rapid redistribution of oxygen in a sandy sediment induced by changes in the flow velocity of the overlying water. Neth. J. Sea Res. **28:** 149–165.

BOUDREAU, B. P., AND OTHERS. 2001. Permeable marine sediments: Overturning an old paradigm. EOS Trans. Am. Geophys. Union **82:** 133–136.

BUCHHOLTZ-TEN BRINK, M. R., G. GUST, AND D. CHAVIS. 1989. Calibration and performance of a stirred benthic chamber. Deep-Sea Res. I **36:** 1083–1101.

CANFIELD, D. E., AND A. TESKE. 1996. Late Proterozoic rise in atmospheric oxygen concentration inferred from phylogenetic and sulphur-isotope studies. Nature **382:** 127–132.

CRAMER, A. 1989. A common artefact in estimates of benthic community respiration caused by the use of stainless steel. Neth. J. Sea Res. **23:** 1–6.

EHRENHAUSS, S., U. WITTE, F. JANSSEN, AND M. HUETTEL. 2004. Decomposition of diatoms and nutrient dynamics in permeable North Sea sediments. Cont. Shelf Res. **24:** 721–737.

EMERY, K. O. 1968. Relict sediments on continental shelves of world. Am. Assoc. Pet. Geol. Bull. **52:** 445–464.

FORSTER, S., M. HUETTEL, AND W. ZIEBIS. 1996. Impact of boundary layer flow velocity on oxygen utilization in coastal sediments. Mar. Ecol. Prog. Ser. **143:** 173–185.

GLUD, R. N., S. FORSTER, AND M. HUETTEL. 1996. Influence of radial pressure gradients on solute exchange in stirred benthic chambers. Mar. Ecol. Prog. Ser. **141:** 303–311.

———, J. K. GUNDERSEN, N. P. REVSBECH, B. B. JØRGENSEN, AND M. HUTTEL. 1995. Calibration and performance of the stirred flux chamber from the benthic lander Elinor. Deep-Sea Res. I **42:** 1029–1042.

———, I. KLIMANT, G. HOLST, O. KOHLS, V. MEYER, M. KUHL, AND J. K. GUNDERSEN. 1999. Adaptation, test and in situ measurements with O_2 microopt(r)odes on benthic landers. Deep-Sea Res. I **46:** 171–183.

GUESS, S. 1998. Oxygen uptake at the sediment-water interface simultaneously measured using a flux chamber method and microelectrodes: Must a diffusive boundary layer exist? Estuar. Coast. Shelf Sci. **46:** 143–156.

HALL, P. O. J., L. G. ANDERSON, M. M. R. VANDERLOEFF, B. SUNDBY, AND S. F. G. WESTERLUND. 1989. Oxygen uptake kinetics in the benthic boundary layer. Limnol. Oceanogr. **34:** 734–746.

HOLST, G., R. N. GLUD, M. KUHL, AND I. KLIMANT. 1997. A microoptode array for fine-scale measurement of oxygen distribution. Sens. Actuat. B **38:** 122–129.

HUETTEL, M., AND G. GUST. 1992*a*. Impact of bioroughness on interfacial solute exchange in permeable sediments. Mar. Ecol. Prog. Ser. **89:** 253–267.

———, AND ———. 1992*b*. Solute release mechanisms from confined sediment cores in stirred benthic chambers and flume flows. Mar. Ecol. Prog. Ser. **82:** 187–197.

———, H. RØY, E. PRECHT, AND S. EHRENHAUSS. 2003. Hydrodynamical impact on biogeochemical processes in aquatic sediments. Hydrobiologia **494:** 231–236.

———, AND A. RUSCH. 2000. Transport and degradation of phytoplankton in permeable sediment. Limnol. Oceanogr. **45:** 534–549.

———, W. ZIEBIS, AND S. FORSTER. 1996. Flow-induced uptake of particulate matter in permeable sediments. Limnol. Oceanogr. **41:** 309–322.

———, ———, ———, AND G. W. LUTHER, III. 1998. Advective transport affecting metal and nutrient distribution and interfacial fluxes in permeable sediments. Geochim. Cosmochim. Acta **62:** 613–631.

JAHNKE, R. A. 2001. Constraining organic matter cycling with benthic fluxes, p. 302–319. *In* B. P. Boudreau and B. B. Jørgensen

[eds.], The benthic boundary layer: Transport processes and biogeochemistry. Oxford Univ. Press.

———, J. R. NELSON, R. L. MARINELLI, AND J. E. ECKMAN. 2000. Benthic flux of biogenic elements on the Southeastern US continental shelf: Influence of pore water advective transport and benthic microalgae. Cont. Shelf Res. **20:** 109–127.

JANSSEN, F., M. HUETTEL, AND U. WITTE. 2005. Pore-water advection and solute fluxes in permeable marine sediments (II): Benthic respiration at three sandy sites with different permeabilities (German Bight, North Sea). Limnol. Oceanogr. **50:** 779–792.

JØRGENSEN, B. B. 2001. Life in the diffusive boundary layer, p. 348–373. *In* B. P. Boudreau and B. B. Jørgensen [eds.], The benthic boundary layer: Transport processes and biogeochemistry. Oxford Univ. Press.

———, AND D. J. DES MARAIS. 1990. The diffusive boundary layer of sediments: Oxygen microgradients over a microbial mat. Limnol. Oceanogr. **35:** 1343–1355.

JULIEN, P. Y. 1995. Erosion and sedimentation. Cambridge Univ. Press.

KLIMANT, I., V. MEYER, AND M. KUHL. 1995. Fiberoptic oxygen microsensors, a new tool in aquatic biology. Limnol. Oceanogr. **40:** 1159–1165.

LI, Y. H., AND S. GREGORY. 1974. Diffusion of ions in sea-water and in deep-sea sediments. Geochim. Cosmochim. Acta **38:** 703–714.

LOHSE, L., E. H. G. EPPING, W. HELDER, AND W. R. VAN RAAPHORST. 1996. Oxygen pore water profiles in continental shelf sediments of the North Sea: Turbulent versus molecular diffusion. Mar. Ecol. Prog. Ser. **145:** 63–75.

MARINELLI, R. L., R. A. JAHNKE, D. B. CRAVEN, J. R. NELSON, AND J. E. ECKMAN. 1998. Sediment nutrient dynamics on the South Atlantic Bight continental shelf. Limnol. Oceanogr. **43:** 1305–1320.

PRECHT, E., U. FRANKE, L. POLERECKY, AND M. HUETTEL. 2004. Oxygen dynamics in permeable sediments with wave-driven pore water exchange. Limnol. Oceanogr. **49:** 693–705.

———, AND M. HUETTEL. 2003. Advective pore-water exchange driven by surface gravity waves and its ecological implications. Limnol. Oceanogr. **48:** 1674–1684.

RASHEED, M., M. I. BADRAN, AND M. HUETTEL. 2003. Influence of sediment permeability and mineral composition on organic matter degradation in three sediments from the Gulf of Aqaba, Red Sea. Estuar. Coast. Shelf Sci. **57:** 369–384.

RASMUSSEN, H., AND B. B. JØRGENSEN. 1992. Microelectrode studies of seasonal oxygen-uptake in a coastal sediment—role of molecular diffusion. Mar. Ecol. Prog. Ser. **81:** 289–303.

SANTSCHI, P. H., R. F. ANDERSON, M. Q. FLEISHER, AND W. BOWLES. 1991. Measurements of diffusive sublayer thicknesses in the ocean by alabaster dissolution, and their implications for the measurements of benthic fluxes. J. Geophys. Res. C **96:** 10641–10657.

SUNDBORG, A. 1956. The river Klaralven; a study of fluvial processes. Geografiska annaler **38:** 125–316.

TENGBERG, A., E. ALMROTH, AND P. O. J. HALL. 2003*a*. Resuspension and its effects on organic carbon recycling and nutrient exchange in coastal sediments: In situ measurements using new experimental technology. J. Exp. Mar. Biol. Ecol. **285:** 119–142.

———, J. HOVDENES, D. BARRANGER, O. BROCANDEL, R. DIAZ, J. SARKKULA, C. HUBER, AND A. STANGELMAYER. 2003*b*. Optodes to measure oxygen in the aquatic environment. Sea Technol. **44:** 10–15.

———, H. STAHL, G. GUST, V. MULLER, U. ARNING, H. ANDERSSON, AND P. O. J. HALL. 2004. Intercalibration of benthic flux chambers I. Accuracy of flux measurements and influence of chamber hydrodynamics. Prog. Oceanogr. **60:** 1–28.

———, AND OTHERS. 1995. Benthic chamber and profiling landers in oceanography—a review of design, technical solutions and functioning. Prog. Oceanogr. **35:** 253–294.

———, AND OTHERS. in press. Intercalibration of benthic flux chambers II. Hydrodynamic characterization and flux comparisons of 14 different designs. Mar. Chem.

THAMDRUP, B., AND D. E. CANFIELD. 2000. Benthic respiration in aquatic sediments, p. 86–103. *In* O. E. Sala, R. B. Jackson, H. A. Mooney, and R. W. Howarth [eds.], Methods in ecosystem science. Springer.

THIBODEAUX, L. J., AND J. D. BOYLE. 1987. Bedform-generated convective transport in bottom sediment. Nature **325:** 341–343.

WHEATCROFT, R. A. 1994. Temporal variation in bed configuration and one-dimensional bottom roughness at the mid shelf STRESS site. Cont. Shelf Res. **14:** 1167–1190.

WILD, C., M. RASHEED, U. WERNER, U. FRANKE, R. JOHNSTONE, AND M. HUETTEL. 2004. Degradation and mineralization of coral mucus in reef environments. Mar. Ecol. Prog. Ser. **267:** 159–171.

WITTE, U., AND O. PFANNKUCHE. 2000. High rates of benthic carbon remineralisation in the abyssal Arabian Sea. Deep-Sea Res. II **47:** 2785–2804.

———, F. WENZHÖFER, S. SOMMER, A. BOETIUS, P. HEINZ, N. ABERLE, M. SAND, A. CREMER, W.-R. ABRAHAM, B. B. JØRGENSEN, AND O. PFANNKUCHE. 2003. In situ experimental evidence of the fate of a phytodetritus pulse at the abyssal sea floor. Nature **424:** 763–766.

ZIEBIS, W., M. HUETTEL, AND S. FORSTER. 1996. Impact of biogenic sediment topography on oxygen fluxes in permeable seabeds. Mar. Ecol. Prog. Ser. **140:** 227–237.

Received: 23 December 2003
Accepted: 18 November 2004
Amended: 28 January 2005